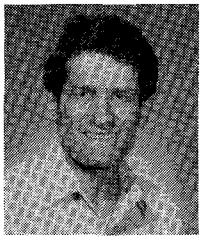

**Barry I. Miller** was born in Chicago, IL, on October 4, 1937. He received the B.S., M.S., and Ph.D. degrees from the University of Chicago, Chicago, IL, in 1959, 1960, and 1966, respectively.

In 1966 he joined Bell Laboratories, Holmdel, NJ, where he has been engaged in research on superconductors, LPE growth of DH GaAs/AlGaAs lasers, MBE growth of GaInAs/InP lasers, and most recently, LPE growth and etching studies of the GaInAsP/InP system for low threshold single-mode lasers and integrated optics.

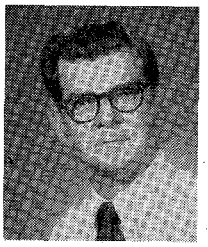

**John A. Rentschler** was born in Kearny, NJ, on January 19, 1934. After completing an enlistment in the U.S. Marine Corps., he attended RCA Institutes.

In 1960 he joined Bell Laboratories, Holmdel, NJ. During the early 1960's he worked on the "Telstar" project. Later, he worked on both silicon and germanium epitaxy and tantalum thin film projects. In 1972, he joined the research area at Bell Laboratories, where he was active in SAW resonator device research. Recently, he has been working with III-V semiconductors for integrated optics.

# Buried Convex Waveguide Structure (GaAl)As Injection Lasers

KATSUHITO SHIMA, KIYOSHI HANAMITSU, AND MASAHITO TAKUSAGAWA

*Abstract*—**The fabrication technique, analysis of the waveguide property, and lasing characteristics of buried convex waveguide structure (BCS) lasers are described. An improved BCS laser structure having a truncated convex active region was produced by using a novel selective etching technique. It was found that the truncated convex waveguide is very effective in suppressing higher order mode lasing when compared with a convex waveguide. The improved BCS lasers showed stable fundamental transverse mode lasing up to 20 mW/facet, typical threshold current of 20 mA, and an external differential quantum efficiency of 28 percent/facet.**

## I. INTRODUCTION

IN the application of injection lasers, linearity of light output-current ($I$-$L$) characteristics and stable fundamental transverse mode lasing are the important characteristics of the lasers. It has become evident in the past few years that laser structures having built-in optical waveguide along the junction plane provide stable transverse mode lasing and the linear $I$-$L$ characteristics. Various kinds of lasers having built-in refractive index distribution along the junction plane have been devised and have been demonstrated to provide stable transverse mode lasing, among which transverse junction lasers [1], rib waveguide lasers [2], buried heterostructure (BH) lasers [3], [4], and channeled substrate buried heterostructure (CSB) lasers [5], [6], are notable examples.

The CSB laser is unique in that it has a convex active region embedded in a lower refractive index material, and built-in refractive index along the junction plane is achieved by the thickness variation of the active region [6]. CSB lasers were first reported by Burnham *et al.* [5] and Kirkby *et al.* [6], and were later modified to improve lasing characteristics [7], [8]. However, it is supposed that CSB lasers do not consistently realize fundamental transverse mode lasing.

Recently, we reported a new type of CSB laser [9], called a buried convex waveguide structure (BCS) laser, which has a narrow active region (3.0-3.5 $\mu$m) and consistently realizes fundamental transverse mode lasing. However, fundamental mode lasing was limited below the output power of 5-6 mW/facet. This may be why the width of the active region is wider than the cutoff width for higher order mode lasing, even in a BCS laser. One possibility for achieving fundamental mode lasing at a higher power level is to make the width of the active region narrower than the cutoff width, but it is difficult to realize such a narrow active region using a GaAs substrate [5], [10]. Another possibility is to realize a waveguide in which there is a large difference in the scattering loss between the fundamental mode and higher order modes to suppress higher order mode lasing [11].

In this paper, we report an improved BCS laser having a truncated convex active region. Its fabrication procedures using a novel selective etching technique and the waveguide analysis are described. In the truncated convex waveguide, the fundamental mode mainly distributes in the center flat region with small loss, but the higher order modes distribute over the tapered region causing large scattering loss. Owing to such waveguide properties, we obtained stable fundamental transverse mode lasing up to 20 mW/facet, a typical threshold current of 20 mA, and an external differential quantum efficiency of 28 percent/facet. It was also found that the out-

Manuscript received March 2, 1982.
The authors are with Fujitsu Laboratories, Ltd., Kawasaki, Japan.

0018-9480/82/1000-1676$00.75 

put beam of the improved BCS laser has no astigmatism over 3.5 times the threshold current.

## II. Structure and Fabrication

### A. Structure

Fig. 1 shows a schematic cross section of the improved BCS laser. In a conventional BCS laser, the active region has a convex cross section [9], but in the improved BCS laser, the active region has a truncated convex cross section which is flat at the center region and tapered toward both sides. The width and thickness of the center region are $2C$ and $d_o$, respectively, and the total waveguide width is $2W$. The active region is completely embedded in the etched channel and aligned with the reverse-biased heterojunction which provides the current confinement to the active region. Each layer in Fig. 1 is typically n-$Ga_{0.7}Al_{0.3}As$ of 0.5 $\mu$m thickness (layer 1), p-$Ga_{0.5}Al_{0.5}As$ of 0.3 $\mu$m thickness (layer 2), n-GaAs of 0.3 $\mu$m thickness (layer 3), n-$Ga_{0.7}Al_{0.3}As$ clad layer (layer 4), p-$Ga_{0.95}Al_{0.05}As$ active region (layer 5), p-$Ga_{0.7}Al_{0.3}As$ clad layer of 1.5 $\mu$m thickness (layer 6), and p-GaAs cap layer of 1 $\mu$m thickness (layer 7). The channel width is typically 4.5 $\mu$m, $2W$ is 3.5 $\mu$m, $2C$ is 2.3 $\mu$m, and $d_o$ is 0.1 $\mu$m.

This truncated convex active region is considered to be divided into two parts: one is the tapered region which is directly influenced by the irregular side walls of the etched channel and is a large scattering loss region; the other is the center flat region which is smooth and is a low-loss region. The fundamental mode mainly distributes in the center low-loss region and higher order modes distribute over the tapered large-loss region, so that suppression of higher order mode lasing is effectively achieved in the truncated convex waveguide.

### B. Fabrication

To obtain the truncated convex active region, we developed a fabrication technique using a novel selective etching. This fabrication technique also enables the control of the buried position of the active region in the etched channel and the growth of a thin active region.

The BCS laser wafers were prepared by a two-step liquid phase epitaxy (LPE) technique. The procedures are shown in Fig. 2. In the first growth stage, a three-layer structure is grown on a (100)-GaAs substrate as shown in Fig. 2(a). The three layers are composed of 1) n-$Ga_{0.7}Al_{0.3}As$, 2) p-$Ga_{0.5}Al_{0.5}As$, and 3) n-GaAs, and they are corresponding to the layers 1-3 in Fig. 1. The GaAs top layer enables the reproducible growth of GaAlAs and GaAs in the second growth stage and also provides a reverse-biased heterojunction for internal current confinement. The $Ga_{0.5}Al_{0.5}As$ layer enables selective etching. After the first growth, 4-5 $\mu$m wide and 2.5 $\mu$m deep channels along the $\langle 01\bar{1}\rangle$ orientation on the wafer were etched by using conventional photolithography [see Fig. 2(b)]. If we take the $\langle 011\rangle$-channels, the GaAlAs at the second growth stage is less reproducibly grown in the channels. The GaAlAs in the second growth stage is less reproducibly grown in the channels when the width of the etched channel is narrower than 4 $\mu$m, even in the $\langle 01\bar{1}\rangle$-channels. Then, small caves were formed in the side wall of the etched channel by using selective etching [Fig. 2(c)]. The $Ga_{1-x}Al_xAs$ is readily dissolved in HF when $x \geq 0.5$, and is not dissolved in HF when $x \leq 0.4$. By applying these etching characteristics, we formed about 0.5 $\mu$m deep caves in the $Ga_{0.5}Al_{0.5}As$ layer on the walls of the etched channels. The selective etching solution used here is composed of $HF:H_3PO_4:H_2O_2 = 800:1200:1$ and the etching time was 30 s at 25°C.

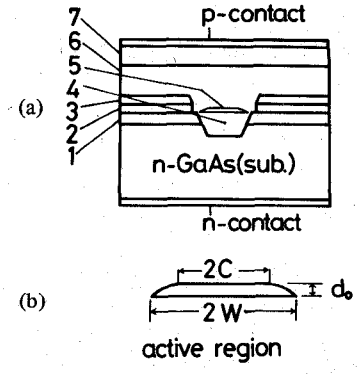


Fig. 1. (a) Schematic cross section of improved BCS laser. Layers are as follows: 1) n-$Ga_{0.7}Al_{0.3}As$, 2) p-$Ga_{0.5}Al_{0.5}As$, 3) n-GaAs, 4) n-$Ga_{0.7}Al_{0.3}As$, 5) p-$Ga_{0.95}Al_{0.05}As$ (active region), 6) p-$Ga_{0.7}Al_{0.3}As$, 7) p-GaAs. (b) Magnified cross section of the truncated convex active region. Total width is $2W$, and the width and thickness of the center flat region are $2C$ and $d_o$, respectively.

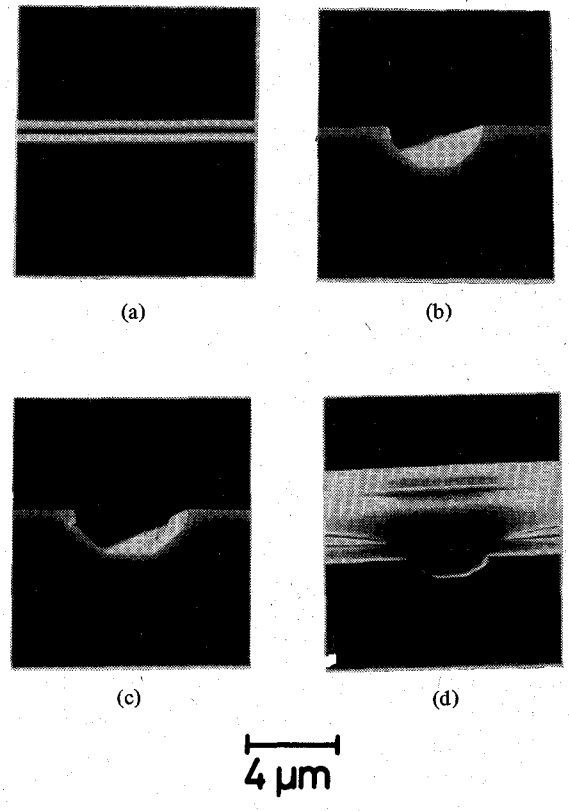


Fig. 2. SEM photographs showing the cross section at each fabrication step. (a) Three-layer structure at first growth stage, (b) after preferential etching, (c) after selective etching, and (d) after second growth.

In the second growth stage, the n-$Ga_{0.7}Al_{0.3}As$ is grown first. When the n-$Ga_{0.7}Al_{0.3}As$ grows to reach the small caves in the side walls of the etched channels, its growth stops at the lower edge of the caves and the growing surface becomes flat. Then, the active region is grown on the flat surface of the n-$Ga_{0.7}Al_{0.3}As$. The active region forms a truncated convex shape by pinning its growth at both sides by the caves. An active region of about $d_o \simeq 0.1$ $\mu$m thickness was reproducibly obtained at a growth time of 20 s at a cooling rate of 0.3°C/min. The thicker active region over 0.15 $\mu$m was rarely obtained, even for a longer growth time. By these growth features, the buried position and the thickness of the active region were automatically determined so that the homogeneous active region along the cavity direction was easily obtained. If the growth time of the n-$Ga_{0.7}Al_{0.3}As$ is sufficiently short, the convex active region is grown. Finally, the p-$Ga_{0.7}Al_{0.3}As$ and p-GaAs layers were grown. The p-$Ga_{0.7}Al_{0.3}As$ can overcome the pinning effect of the small caves for a long period of the growth time so that it fills the channels completely [Fig. 2(d)]. It was observed that there was a relation of $2C \simeq (2W)2/3$ when $3 \leqslant 2W \leqslant 4$ $\mu$m and $d_o \simeq 0.1$ $\mu$m.

Lasers having a cavity length of 200 $\mu$m were fabricated from the wafers and, for CW operation, a sample was bonded on to a diamond heat sink using an AuSn alloy bonding solder.

### C. Discussion

The growth characteristics of the filling of the etched channels are quite different from the results reported previously [8], [10], [12] because of the existence of the GaAlAs layers and the small caves formed in the side walls of the etched channels.

The three-layer structure in the first growth stage enables production of a narrow active region by eliminating melt-back of the shoulder of the etched channels, carrier leak to the GaAs substrate, and absorption of lasing light in the GaAs substrate by keeping a distance between the active region and the substrate. However, the minimum width of the active region reproducibly obtained was about 3 $\mu$m. The channels remained without the LPE growth if the channels were narrower than 4 $\mu$m (corresponding to $2W < 3$ $\mu$m), and the channels also remained, even though the channels were wider than 4 $\mu$m when we took the ⟨011⟩-channels. It is difficult to grow the air-exposed surface of GaAlAs directly, and the LPE growth should begin from the GaAs at the bottom of the channels [3]. If the width of the channels is narrower than 4 $\mu$m, the melts cannot fill the channels completely because of surface tension of the melts. In the case of the ⟨011⟩ channels, dovetail channels were formed. The GaAlAs at the shoulder of the dovetail channels prevents the melts from filling the channels.

The truncated convex active region was realized by using selective etching. It is possible to obtain an LPE growth on an inclined surface of the air-exposed GaAlAs, but it is difficult on a flat surface [3]. Therefore, the LPE growth is pinned at the lower edges of the caves at which nearly a flat GaAlAs surface appears, and the growth rate becomes extremely slow.

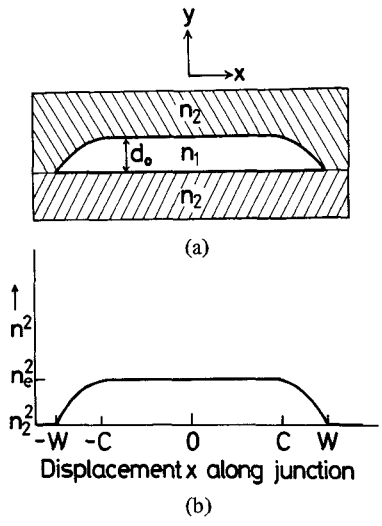


Fig. 3. (a) Schematic cross section of the truncated convex waveguide and (b) the corresponding effective dielectric constant profile along the junction plane.

The buried position of the active region in the channels is semiautomatically determined by the caves and is almost independent of the growth time so that it is constant along the cavity direction. The growth rate of the active region is also slow, so we can easily obtain a thin active region of 0.08-0.12 $\mu$m.

## III. Waveguide Properties

### A. Analysis

Fig. 3(a) shows the schematic cross section of the truncated convex waveguide and the coordinate system used. To simplify the analysis, we assume that 1) the active region (refractive index of $n_1$) is buried in the uniform refractive index material (refractive index of $n_2$), 2) the thickness of the active region ($d(x)$) is constant ($d_o$) in the center region and decreases gradually to zero on both sides, and 3) only the electric field along the junction plane (TE mode) is considered.

The transverse mode behavior can be analyzed by means of the effective refractive index approximation [13]. In this approximation, the eigenmodes are given by the product of two functions, $E_x(x)$ and $E_x(y)$, and we have the following separated wave equations [14]:

$$\left\{\frac{d^2}{dx^2} + (k^2 n_e(x)^2 - \beta^2)\right\} E_x(x) = 0 \tag{1}$$

$$\left\{\frac{d^2}{dy^2} + (k^2 n_o(y)^2 - n_e^2)\right\} E_x(y) = 0 \tag{2}$$

where

$$n_o(y)^2 = \begin{cases} n_1^2 & |y| \leqslant d_o/2 \\ n_2^2 & |y| > d_o/2 \end{cases} \tag{3}$$

$k = 2\pi/\lambda$ is the free-space propagation constant, $\lambda$ is the free-space wavelength, $\beta$ is the propagation constant of the guided wave in the $z$ direction, $n_e$ is the effective refractive index for mode with respect to the $y$ direction determined by solving (2), and $n_e(x)$ is the effective refractive index along the $x$

direction. The resulting modes of $E_x(y)$ have a usual cosinusoidal with exponential tail variation.

The thickness of the active region $d(x)$ can be approximately expressed [6] as

$$d(x) = \begin{cases} d_o & |x| \leqslant C \\ d_o \left\{1 - \left(\dfrac{x - C}{W - C}\right)^2\right\} & C < |x| \leqslant W \\ 0 & |x| > W. \end{cases} \tag{4}$$

The effective refractive index of the waveguide $n_e(x)$ is expressed as

$$n_e(x)^2 = n_2^2 + P^2(n_1^2 - n_2^2) \tag{5}$$

where $P$ is the normalized propagation constant in the $y$ direction [15]. If $d(x)$ is thin, we can approximate [16] as

$$P \simeq \tfrac{1}{2}\, d(x)\, k \sqrt{n_1^2 - n_2^2}. \tag{6}$$

Using (4)-(6) and neglecting higher order terms, we obtain the effective refractive index profile along the $x$ direction as

$$n_e(x)^2 \begin{cases} n_e^2 & |x| \leqslant C \\ = n_e^2 \left\{1 - \dfrac{n_e^2 - n_2^2}{n_e^2}\left(\dfrac{x - C}{W - C}\right)^2\right\} & C < |x| \leqslant W \\ n_2^2 & |x| > W. \end{cases} \tag{7}$$

$n_e(x)^2$ is illustrated in Fig. 3(b).

The transverse mode behavior is now obtained by substitution of the effective refractive index profile along the $x$ direction (7) into the wave equation (1). To solve (1), we applied a simplified series solution method developed by Dil *et al.* [17] and Gambling *et al.* [18] for optical fiber analysis and later applied it to a cladded parabolic index waveguide by Adams [19]. Table I gives the expression for the field distributions and eigenvalue equations obtained by this method, and the corresponding result for a convex waveguide approximated as a cladded parabolic index profile [19], [20] is also shown. The notation in Table I uses the normalized variables [21]-[23]. It is found that the convergence of the series was such that an adequate degree of accuracy was achieved in about 20 terms for the center region and 50 terms for the tapered region.

Far-field distribution of the emitted laser beam is also calculated using the results for $E_x(x)E_x(y)$. The beam profiles parallel to the junction plane were calculated by the approximate formula [24]

$$I(\theta_x) \propto (1 + \cos\theta_x)^2 \left| \int_{-\infty}^{\infty} E_x(x) \exp(j \sin\theta_x kx)\, dx \right|^2 \tag{8}$$

where $\theta_x$ is measured from the normal to the mirror facet.

### *B. Calculated Results and Discussion*

Fig. 4 shows an example of the calculated results, where the curves give the cutoff conditions, the abscissa and the ordinate being the width $2W$, and the thickness $d_o$ of the active region in the center region, respectively. The parameters used are $n_1 = 3.62$, $n_2 = 3.4$, and $\lambda = 850$ nm. The relation of $C = 2W/3$, which is observed in the range of $3 \leqslant 2W \leqslant 4$ ($\mu$m), is assumed in all the values of $2W$. Near the origin, all the higher order modes are cutoff, and only the fundamental mode is allowed. From the active region shape, it is expected that the truncated convex waveguide has the properties between the BH (rectangular) waveguide and the convex waveguide according to the values of $2C$. Fig. 5 shows the cutoff condition at the finite width of $2W = 3.5$ $\mu$m for the first-order mode as a function of $2C$. This corresponds to the BH waveguide at $2C = 2W$ and to the convex waveguide at $2C = 0$.

The lasers with built-in refractive index distribution along the junction plane experimentally show fundamental transverse mode lasing at low power levels for values of $2W$ that allow higher order modes [3], [4], [9]. The scattering loss from the irregular boundaries of the guide walls is very effective for suppression of higher order mode lasing, thus keeping the fundamental mode lasing up to higher power levels [11]. Fig. 6 shows the transverse mode confinement factors for the fundamental mode and the first-order mode in the truncated convex waveguide. The dashed curves show the confinement factor $\Gamma_m$ ($m = 0$ for fundamental mode and $m = 1$ for the first-order mode) for the entire waveguide width $2W$ and the solid curves show the confinement factors $\Gamma'_m$ for the center region $2C$. There is no particular difference in $\Gamma_m$ ($\simeq 1$) between the fundamental mode and the first-order mode when $2W \geqslant 3$ $\mu$m. Therefore, the fundamental mode, as well as the first-order mode, can oscillate if there is no difference in the loss between them. On the other hand, there is a particular difference in $\Gamma'_m$ between the fundamental mode and the first-order mode even though $2W \geqslant 3$ $\mu$m, and higher order modes distribute over the tapered region. If there is a large scattering loss in the tapered region, the transverse mode is stabilized by this scattering loss. To estimate the scattering loss in the tapered region, we compare the threshold current of the lasers having the truncated convex waveguide with that of the lasers having the convex waveguide. The calculated field distributions of the fundamental transverse modes in the truncated convex waveguide and in the convex waveguide are shown in Fig. 7. The field in the truncated convex waveguide distributes more widely than that in the convex waveguide, so the influence of the irregular boundaries of the guide walls is larger in the truncated convex waveguide than in the convex waveguide, which causes the higher threshold current. Actually, the average threshold current of the lasers having the truncated convex waveguide was 20 mA, and that of the lasers having the convex waveguide was 16 mA as described in Section IV. Therefore, the fundamental mode in the truncated convex waveguide is somewhat influenced by the scattering loss in the tapered region and this scattering loss is supposed to be fairly large. The scattering loss due to the irregular boundaries of the guide walls may have the relation [11], [24]

$$\alpha(m) \propto (m + 1)^2$$

where $m$ is the transverse mode number ($= 0, 1, 2, \cdots$). The scattering loss rapidly increases with the mode number and

TABLE I
THE WAVEGUIDE MODELS AND MATHEMATICAL DETAILS OF THEIR SOLUTIONS

| | Convex waveguide | Truncated convex waveguide |
|---|---|---|
| Parameters | $u^2=W^2(k^2n_e^2-\beta^2)$<br>$v^2=W^2k^2(n_e^2-n_2^2)$<br>$\omega^2=v^2-u^2$ | $u^2=C^2(k^2n_e^2-\beta^2)$<br>$u'^2=(W-C)^2(k^2n_e^2-\beta^2)$<br>$v'^2=(W-C)^2k^2(n_e^2-n_2^2)$<br>$\omega^2=v'^2-u'^2$ |
| Dielectric profile: $n_e(x)^2$ | $n_e^2(1-\frac{n_e^2-n_2^2}{n_e^2}(\frac{x}{W})^2)$ $(\lvert x\rvert\le W)$<br>$n_2^2$ $(\lvert x\rvert>W)$ | $n_e^2$ $(\lvert x\rvert\le C)$<br>$n_e^2(1-\frac{n_e^2-n_2^2}{n_e^2}(\frac{\lvert x\rvert-C}{W-C})^2)$ $(C<\lvert x\rvert\le W)$<br>$n_2^2$ $(\lvert x\rvert>W)$ |
| Field distribution $E_x(x)$ | $\sum_{n=0}^{N} a_n(\frac{x}{W})^n$ $(\lvert x\rvert\le W)$<br>$(\sum_{n=0}^{N} a_n)\, e^{\omega}(1-\frac{\lvert x\rvert}{W})$ $(\lvert x\rvert>W)$<br>$a_n=\frac{v^2a_{n-4}-u^2a_{n-2}}{n(n-1)}$<br>Even order modes, $a_0=1, a_{2i+1}=0$<br>odd order modes, $a_1=1$, $a_{2i}=0$ (all i) | $\sum_{n=0}^{N} a_n(\frac{x}{C})^n$ $(\lvert x\rvert\le C)$<br>$\sum_{m=0}^{M} b_m(\frac{\lvert x\rvert-C}{W-C})^m$ $(C<\lvert x\rvert\le W)$<br>$(\sum_{m=0}^{M} b_m)\, e^{\omega}(\frac{W-\lvert x\rvert}{W-C})$ $(\lvert x\rvert>W)$<br>$a_n=\frac{-u^2a_{n-2}}{n(n-1)}$<br>$b_m=\frac{v'^2b_{m-4}-u'^2b_{m-2}}{m(m-1)}$ |
| Eigen value equation | $\sum_{n=1}^{N} na_n=-\omega\sum_{n=0}^{N} a_n$ | $\sum_{n=1}^{N} na_n=\frac{C\,b_2}{W-C}$<br>$\sum_{m=1}^{M} mb_m=-\omega\sum_{m=0}^{M} b_m$ |

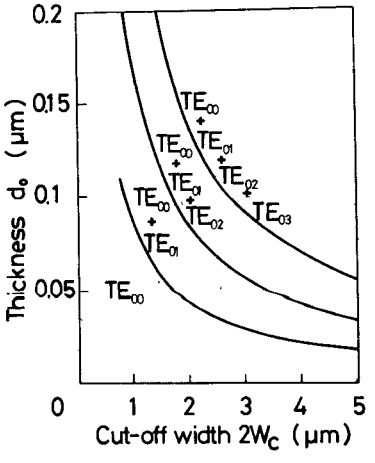


Fig. 4. Cutoff condition of the low-order transverse modes as a function of the width $2W$ and the thickness $d_o$ with the relation of $C = 2W/3$.

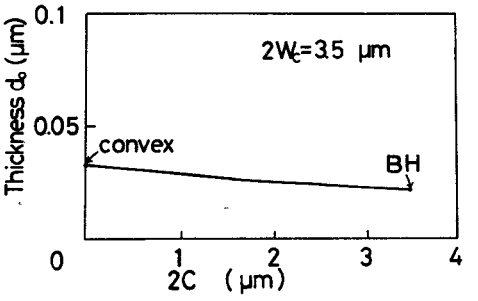


Fig. 5. Cutoff condition of the first-order transverse mode as a function of $2C$ and $d_o$ when the total width $2W = 3.5$ μm.

higher order mode lasing is effectively suppressed in the truncated convex waveguide.

## IV. DEVICE CHARACTERISTICS

### A. Comparison of BCS Lasers Having a Convex and a Truncated Convex Active Region

Two types of BCS lasers were produced: one has a convex active region, which is the same as a conventional structure; and the other is an improved structure having a truncated convex active region. The average and lowest pulsed threshold current for the lasers having a convex active region were

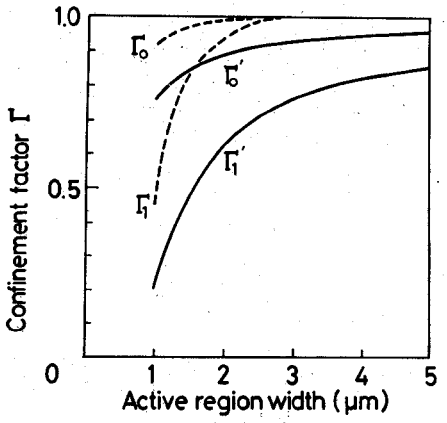


Fig. 6. The transverse mode confinement factors for the fundamental mode and the first-order mode. Dashed curves are the confinement factors for the total width $2W$ ($\Gamma_0$ for the fundamental mode and $\Gamma_1$ for the first-order mode), and solid curves are the confinement factors for center flat region $2C$ ($\Gamma'_0$ for the fundamental mode and $\Gamma'_1$ for the first-order mode).

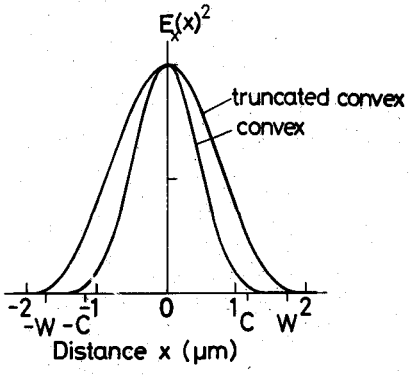


Fig. 7. The field intensity distributions in the truncated convex waveguide and the convex waveguide for $2W = 3.5$ μm, $d_o = 0.1$ μm, and $2C = 2.3$ μm (only for the truncated convex waveguide), and $\lambda = 850$ nm.

16 and 9 mA, respectively, and those for the improved lasers were 20 and 14 mA, respectively. The threshold current is extremely reduced as compared with that obtained before, which was 25 mA (average) [9]. These results show that the fabrication technique developed in this paper gives the homogeneous active region. Higher threshold current of the improved lasers as compared with that of the lasers having a convex active region can be caused by the difference of the scattering loss as described in Section III.

Fig. 8 shows typical far-field patterns along the junction plane at various power levels and the photographs of the corresponding lasers. These lasers had almost the same $d_o$ (~0.12 μm), $2W$ (~3.7 μm), and $\lambda$ (~850 nm), except the shape of the active region. The improved laser shows the stable fundamental mode lasing over 10 mW/facet [Fig. 8(a)], whereas the laser having a convex active region shows the transverse mode deformation over 6 mW/facet [Fig. 8(b)]. The beam divergence of the lasers having a convex active region was wider than that of the improved lasers. The beam divergence (measured at half-power points) of the lasers having a convex active region was 20-30° and was less controllable. On the other hand, we can reproducibly obtain a beam divergence of 14-18° in the improved lasers.

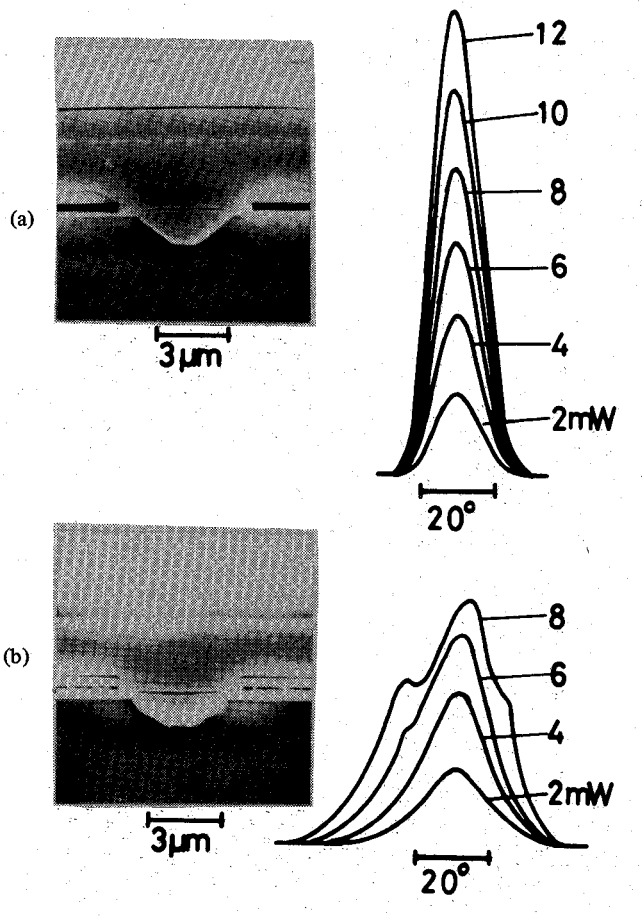


Fig. 8. The far-field patterns along the junction plane at various power levels and the SEM photographs of the corresponding lasers. (a) The laser having a truncated convex waveguide: $2W = 3.7$ μm, $2C = 2.2$ μm, $d_o = 0.12$ μm, and $\lambda = 848$ nm. (b) The laser having a convex waveguide: $2W = 3.7$ μm, $d_o = 0.11$ μm, and $\lambda = 852$ nm.

### *B. BCS Lasers Having Truncated Convex Active Region*

Fig. 9 shows typical CW *I-L* characteristics. The threshold current was typically 20 mA, and the lowest threshold was 15 mA (CW). Such a low threshold was achieved by the very effective current confinement and the homogeneous active region along the cavity direction. The *I-L* characteristics were extremely linear with no kinks up to 20 mW/facet, and the external differential quantum efficiency was about 28 percent/facet. Fig. 10 shows typical far-field distribution under CW operation. The transverse mode was stabilized up to 20 mW/facet; however, at a power level of 25 mW/facet, the field distribution became slightly deformed. It is considered that suppression of the higher order modes is ineffective, even in the truncated convex waveguide at power levels over 20 mW/facet. Fig. 11 shows the experimental results of the beam divergence parallel to the junction plane as a function of the active region thickness $d_o$ and also shows the calculated curve. The experimental results are slightly larger than the theoretical prediction when $d_o$ becomes thicker. This may be why the center region is not flat, but slightly curved, and the curvature becomes larger as $d_o$ becomes thicker, resulting in a larger beam divergence. The beam divergence along the junction plane was 14-18° when $0.08 \leqslant d_o \leqslant 0.12$ μm, which was reproducibly obtained in this experiment.

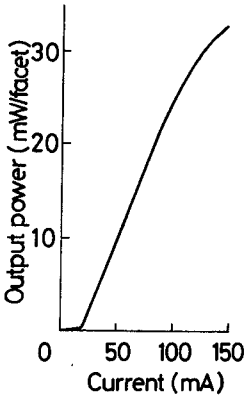


Fig. 9. Typical CW $I$–$L$ characteristics of the improved BCS laser.

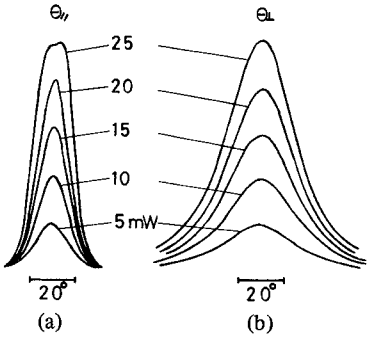


Fig. 10. Far-field patterns at various power levels under CW operation of the improved BCS laser. (a) Parallel to the junction plane. (b) Perpendicular to the junction plane.

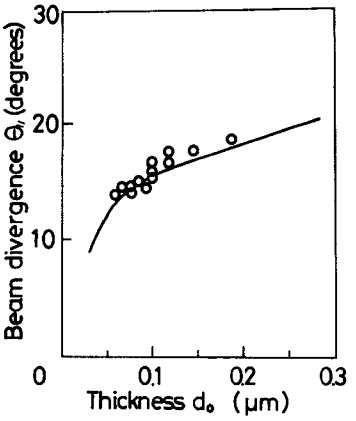


Fig. 11. Beam divergence parallel to the junction plane as a function of the active region thickness $d_O$ for the lasers with $3.2 \leqslant 2W \leqslant 3.8$ $\mu$m. The solid curve is calculated beam divergence for $2W = 3.5$ $\mu$m, $2C = 2.3$ $\mu$m by using (8).

Fig. 12 shows a typical lasing spectra at various current levels. Single longitudinal mode lasing starts to become dominant at slightly above threshold.

In applications for an astigmatically corrected optical system, the stable field distribution as well as astigmatism are important characteristics of the lasers, and it is desirable that the beam-waist position be independent of the excitation levels. The dependences of beam width and the beam-waist position on various current levels were examined by measuring

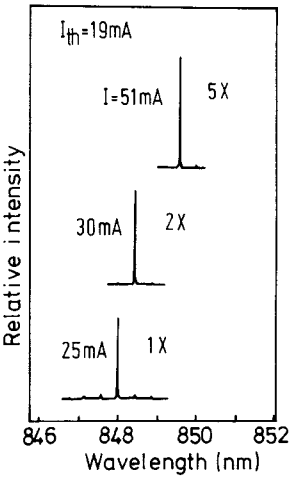


Fig. 12. Lasing spectra at various current levels.

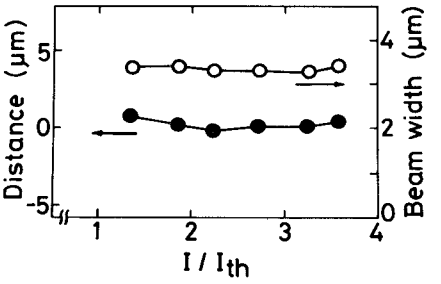


Fig. 13. Dependence of full beam width at $1/e^2$ points (○) and distance between the beam waist position parallel to the junction plane and that perpendicular to the junction plane (●) on current levels.

the near-field patterns as shown in Fig. 13. Open circles show full beam width at $e^{-2}$ points parallel to the junction. The beam width maintained a constant value over 3.5 times the threshold current. The solid circles show the dependence of the distance between the beam waist position parallel to the junction and that perpendicular to the junction. The distance is nearly zero, and this coincidence is a result of refractive index guiding [26] in a truncated convex waveguide. The output beam of the BCS laser has no astigmatism over 3.5 times the threshold current.

## V. Conclusion

Buried convex waveguide structure (BCS) lasers were fabricated by using a novel selective etching technique. The fabrication technique developed in this paper realizes a truncated convex waveguide and provides the reproducible growth of a thin active region (0.08–0.12 $\mu$m) and a homogeneous active region along the cavity direction.

The mode-guiding mechanism and the lasing characteristics of BCS lasers having a truncated convex active region are also described. These lasers achieve fundamental transverse mode lasing up to 20 mW/facet (CW) by effectively suppressing the higher order modes. The threshold current was typically 20 mA (CW) and the external differential quantum efficiency was 28 percent/facet. The output beam of the BCS laser having a truncated convex waveguide has no astigmatism over 3.5 times the threshold.

## ACKNOWLEDGMENT

The authors wish to thank Dr. T. Misugi, Dr. K. Dazai, Dr. Y. Tohyama, Dr. K. Hori, and Dr. T. Fujiwara for their encouragement. They also wish to thank S. Ohsaka, T. Fukuda, N. Takagi, K. Segi, and T. Tabuchi for their useful discussions and their cooperation in device fabrication, and Dr. H. Ishikawa and Dr. K. Wakao for their helpful discussions.

## REFERENCES

[1] H. Namizaki, H. Kan, M. Ishii, and A. Ito, "Characteristics of junction-stripe-geometry laser diode," *Japan. J. Appl. Phys.*, vol. 13, pp. 1618–1623, Oct. 1974.

[2] T. P. Lee, C. A. Burrus, B. I. Miller, and R. A. Logan, "$Al_xGa_{1-x}As$ double-heterostructure rib-waveguide injection laser," *IEEE J. Quantum Electron.*, vol. QE-11, pp. 432–435, July 1975.

[3] T. Tsukada, "GaAs-$Ga_{1-x}Al_xAs$ buried-heterostructure injection lasers," *J. Appl. Phys.*, vol. 45, pp. 4899–4906, Nov. 1974.

[4] K. Saito and R. Ito, "Buried-heterostructure AlGaAs lasers," *IEEE J. Quantum Electron.*, vol. QE-16, pp. 205–215, Feb. 1980.

[5] R. D. Burnham and D. R. Scifre, "Etched buried heterostructure GaAs/GaAlAs injection lasers," *Appl. Phys. Lett.*, vol. 27, pp. 510–511, Nov. 1975.

[6] P. A. Kirkby and G. H. Thompson, "Channeled substrate buried heterostructure GaAs-(GaAl)As injection lasers," *J. Appl. Phys.*, vol. 47, pp. 4578–4589, Oct. 1976.

[7] L. Figueroa and S. Wang, "Inverted-ridge-waveguide double-heterostructure injection laser with current and lateral optical confinement," *Appl. Phys. Lett.*, vol. 31, pp. 45–47, 1977.

[8] P. A. Kirkby, "Channeled-substrate narrow-stripe GaAs/GaAlAs injection lasers with extremely low threshold currents," *Electron. Lett.*, vol. 15, pp. 824–826, Dec. 1979.

[9] K. Shima, K. Hanamitsu, T. Fujiwara, and M. Takusagawa, "Buried convex waveguide structure (GaAl)As injection lasers," *Appl. Phys. Lett.*, vol. 38, pp. 605–607, Apr. 1981.

[10] K. Funakoshi, A. Doi, K. Aiki, and R. Ito, "Liquid-phase epitaxial growth of $Ga_{1-x}Al_xAs$ on channeled substrate," *J. Crystal Growth*, vol. 45, pp. 252–256, 1978.

[11] Y. Suematsu and M. Yamada, "Transverse mode control in semiconductor lasers," *IEEE J. Quantum Electron.*, vol. QE-9, pp. 305–311, Feb. 1973.

[12] D. Botez, W. T. Tsang, and S. Wang, "Growth characteristics of GaAs-$Ga_{1-x}Al_xAs$ structure fabricated by liquid-phase epitaxy over preferentially etched channels," *Appl. Phys. Lett.*, vol. 234–236, Feb. 1976.

[13] E. A. Marcatili, "Dielectric rectangular waveguide and directional coupler for integrated optics," *Bell Syst. Tech. J.*, vol. 48, pp. 2071–2102, Sept. 1969.

[14] T. Suhara, Y. Handa, H. Nishihara, and J. Koyama, "Analysis of optical channel waveguides and directional coupler with graded-index profile," *J. Opt. Soc. Amer.*, vol. 69, pp. 807–815, June 1979.

[15] W. W. Anderson, "Mode confinement and gain in junction lasers," *IEEE J. Quantum Electron.*, vol. QE-1, pp. 228–236, June 1965.

[16] D. P. Dumke, "The angular beam divergence in double-heterojunction lasers with very thin active regions," *IEEE J. Quantum Electron.*, vol. QE-11, pp. 400–402, July 1975.

[17] J. G. Dil and H. Blok, "Propagation of electromagnetic surface wave in a radially in homogenious optical waveguide," *Opt. Electron.*, vol. 4, pp. 415–428, Sept. 1973.

[18] W. A. Gambling, D. N. Payne, and H. Matsumura, "Cut-off frequency in radially inhomogeneous single-mode fiber," *Electron. Lett.*, vol. 13, pp. 139–140, Mar. 1977.

[19] M. J. Adams, "The cladded parabolic-index profile waveguide: Analysis and application to stripe-geometry lasers," *Opt. Quantum Electron.*, vol. 10, pp. 17–29, Jan. 1978.

[20] E. Oomura, T. Murotani, H. Higuchi, H. Namizaki, and W. Susaki, "Low threshold InGaAsP/InP buried crescent laser with double current confinement structure," *IEEE J. Quantum Electron.*, vol. QE-17, pp. 646–650, May 1981.

[21] W. O. Schlosser, "Gain-induced modes in planar structures," *Bell Syst. Tech. J.*, vol. 52, pp. 887–905, July–Aug., 1973.

[22] G. B. Hocker and W. K. Burns, "Mode dispersion in diffused channel waveguides by the effective index method," *Appl. Opt.*, vol. 16, pp. 113–118, Jan. 1977.

[23] H. Kogelnik and V. Ramaswamy, "Scaling rules for thin-film optical waveguides," *Appl. Opt.*, vol. 13, pp. 1857–1862, Aug. 1974.

[24] P. J. DeWaard, "Calculation of the far-field half-power width and mirror reflection coefficients of double-heterostructure lasers," *Electron. Lett.*, vol. 11, pp. 11–12, Jan. 1975.

[25] Y. Suematsu and K. Furuya, "Radiation conversion losses and resonance of dielectric waveguide," in *Proc. Meet. Inst. Electron. Commun. Eng. Japan*, vol. QE-72-21, June, 1972.

[26] C. Chen and S. Wang, "Near-field and beam-waist position of the semiconductor laser with a channeled-substrate planar structure," *Appl. Phys. Lett.*, vol. 37, pp. 257–260, Aug. 1980.

**Katsuhito Shima** was born in Hokkaido, Japan, on December 8, 1948. He received the B.E., M.E., and Ph.D. degrees in electronic engineering from Hokkaido University, Sapporo, Japan, in 1971, 1973, and 1976, respectively.

In 1977 he joined Fujitsu Laboratories, Ltd., Kawasaki, Japan, where he has been engaged in the research and development of semiconductor lasers.

Dr. Shima is a member of the Institute of Electronics and Communication Engineers of Japan and the Japan Society of Applied Physics.

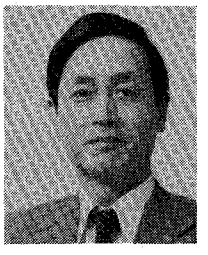

**Kiyoshi Hanamitsu** was born in Wakayama, Japan, on October 16, 1945. He received the B.E., M.E., and Ph.D. degrees in electrical engineering from Osaka University, Osaka, Japan, in 1968, 1970, and 1976, respectively.

In 1976 he joined Fujitsu Laboratories, Ltd., Kawasaki, Japan, where he has been engaged in the research and development of semiconductor lasers.

Dr. Hanamitsu is a member of the Institute of Electronics and Communication Engineers of Japan and the Japan Society of Applied Physics.

**Masahito Takusagawa** was born in Kofu, Japan, on June 6, 1940. He received the B.E., M.E., and Ph.D. degrees in electronic engineering from Tohoku University, Sendai, Japan, in 1963, 1965, and 1968, respectively.

In 1968 he joined the Semiconductor Research Institute, Sendai, Japan, where he was engaged in the research on the GaAs laser. In 1971, he joined Fujitsu Laboratories, Ltd., Kawasaki, Japan, where he has been engaged in the research and development of semiconductor lasers for optical fiber transmission and optical information processing. Currently, he is a Deputy Manager of the Optical Semiconductor Devices Laboratory, Semiconductor Division, Fujitsu Laboratories.

Dr. Takusagawa is a member of the Institute of Electronics and Communication Engineers of Japan and the Japan Society of Applied Physics.